

# Domain-Wall Induced Quark Masses in Topologically-Nontrivial Background

Valeriya Gadiyak, Xiangdong Ji, Chulwoo Jung  
*Department of Physics*  
*University of Maryland*  
*College Park, Maryland 20742*

(UMD PP#00-055 DOE/ER/40762-201 February 2000)

## Abstract

In the domain-wall formulation of chiral fermion, the finite separation between domain-walls ( $L_s$ ) induces an effective quark mass ( $m_{\text{eff}}$ ) which complicates the chiral limit. In this work, we study the size of the effective mass as the function of  $L_s$  and the domain-wall height  $m_0$  by calculating the smallest eigenvalue of the hermitian domain-wall Dirac operator in the topologically-nontrivial background fields. We find that, just like in the free case,  $m_{\text{eff}}$  decreases exponentially in  $L_s$  with a rate depending on  $m_0$ . However, quantum fluctuations amplify the wall effects significantly. Our numerical result is consistent with a previous study of the effective mass from the Gell-Mann-Oakes-Renner relation.

arXiv:hep-lat/0002023v2 22 Mar 2000

Chiral symmetry and its explicit and/or spontaneous breakings are important aspects of strong interaction phenomenology. Chiral dynamics dominates the low-energy hadron structure and interactions. The chiral phase transition at finite temperature has been sought after experimentally for a long time. In addition, the weak interaction probes couple directly to the chiral currents, and the matrix elements of which sensitively depend on the chiral properties of hadron systems. On the theoretical frontier, however, massless fermions defy the naive nonperturbative treatments. Indeed, for more than two decades, finding an appropriate fermion formulation has been one of the most difficult challenges in lattice quantum chromodynamics (QCD). In the last few years, Kaplan and Shamir's domain-wall construction [1,2] and Narayanan and Neuberger's overlap fermion formalism [3] have emerged as promising approaches to simulating massless quarks. In this paper, we aim to study the effectiveness of the domain-wall approach which has already been used in a number of realistic numerical investigations [4–6].

Following previous studies, we adopt Shamir's version of the domain wall fermion formulation [2], in which the five dimensional Wilson fermion is first introduced. The finite fifth dimension with  $L_s$  lattice sites extends from  $s = 0$  to  $s = L_s - 1$ . Dirichlet boundary condition on the quark fields is applied to the four-dimensional slices at  $s = -1$  and  $s = L_s$ . The fifth component of the gauge potential is identically zero and the other four components are the same at every  $s$  slice. The above construction in the gauge-field-free case yields nearly-massless modes when the negative Wilson mass  $m_0$  (the wall height) is taken between 0 and 10. These chiral fermions appear as the surface modes at  $s = 0$  and  $s = L_s - 1$  with opposite chirality. For  $0 < m_0 < 2$ , one flavor Dirac fermion can be constructed as

$$\psi(n) = P_+ \psi(n, s = 0) + P_- \psi(n, s = L_s - 1) , \quad (1)$$

where  $P_{\pm} = (1 \pm \gamma_5)/2$  are the chiral projection operators and  $n$  labels four-dimensional lattice sites. For the finite wall separation ( $L_s \neq \infty$ ), the chiral mode on the  $s = 0$  wall couples with the one with the opposite chirality on the  $s = L_s - 1$  wall in an exponentially small way. Because of this coupling, a finite residual fermion mass is produced. The goal of this paper is to understand the size and dependence of this induced fermion mass on  $m_0$ ,  $L_s$  when realistic background gauge fields are introduced.

In the absence of the gauge potentials, the effective mass can be defined in terms of the pole of the free Green's function. For a large  $L_s$ , it has a simple analytical form [2],

$$m_{\text{eff}} = m_0(2 - m_0)(1 - m_0)^{L_s} . \quad (2)$$

One can also obtain  $m_{\text{eff}}$  by either diagonalizing the hermitian domain-wall Dirac operator  $H_{DW} = \gamma_5 P_s D$  or  $D^\dagger D = H_{DW}^2$  [2,5], where  $D$  is the domain-wall Dirac operator and  $P_s$  is the reflection along the fifth dimension. On a lattice with the periodic boundary condition, the lowest four-momentum of a fermion is zero, and the lowest eigenvalue of  $\gamma_5 P_s D$  is just  $m_{\text{eff}}$ . To study the effective mass in an external gauge field, we have constructed a code to diagonalize  $H_{DW}$  numerically. To test the code, we have computed  $m_{\text{eff}}$  on an  $8^4$  lattice with  $L_s = 8, 12$ , and  $16$ , and the result is shown in Fig. 1 together with the exact answer from Eq. (1). An ideal massless fermion is obtained at  $m_0 = 1$  where  $m_{\text{eff}}$  vanishes identically. For  $m_0 \neq 1$ , the induced quark mass decays exponentially in  $L_s$  with a rate depending strongly on  $m_0$ . The exponential decay slows down significantly as  $m_0$  approaches 0 and 2. For any given accuracy  $\epsilon$  and any  $L_s$ , there is a window surrounding  $m_0 = 1$  in which  $m_{\text{eff}} < \epsilon$ .

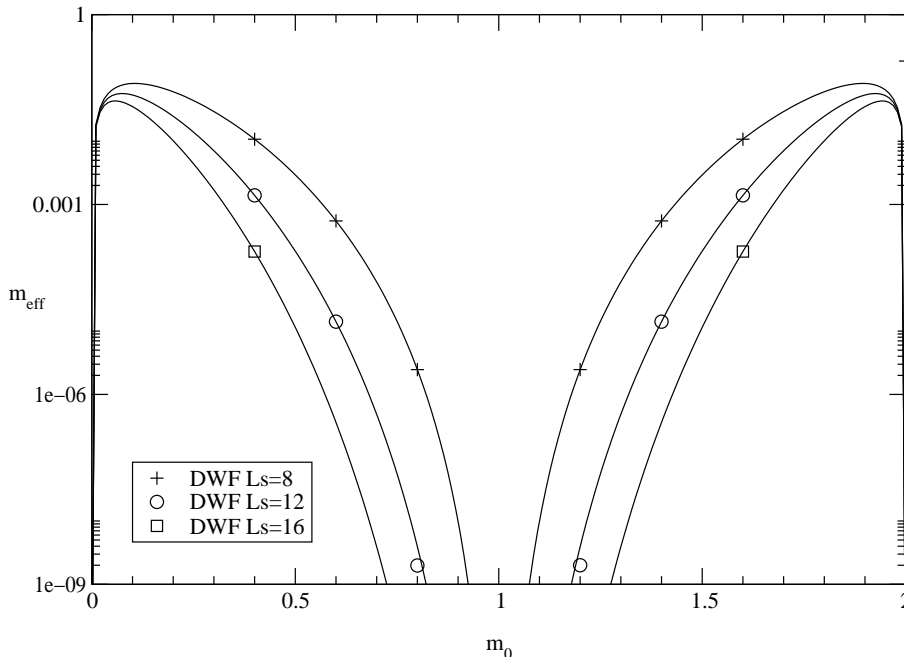


FIG. 1. Effective quark mass induced by domain-walls for the free field configuration.  $L_s$  is the number of lattice sites in the fifth direction.

In the presence of a realistic gauge potential, the effective quark mass result from the finite wall separation may depend on how it is defined. Different definitions shall yield results consistent up to a factor of order unity. One approach is to exploit the explicit quark mass dependence in chiral Ward identities such as the Gell-Mann-Oakes-Renner (GMOR) relation as done in Ref. [7]. Here we explore the effective mass in an alternative way. In continuum field theory, the Atiyah-Singer theorem [8] states that the Dirac operator has a zero eigenvalue in the presence of an external background with topological charge  $|Q| = 1$ . The explicit form of the solution was found by 't Hooft in 1976 [9]. On the lattice, however, the notion of topological charge is ill defined: any gauge configuration can be continuously deformed into a null gauge field. Moreover, the discretization of an instanton field can introduce finite lattice-spacing effects lifting any exact zero eigenvalue. Therefore, a test of the Atiyah-Singer theorem on lattice is usually complicated with various lattice artifacts.

There exists, however, a definition of lattice topology and fermion zero mode which largely avoids this complication. In the overlap formalism, the Dirac operator is constructed from the overlap of two many-fermion ground states [3]. According to their recipe, one starts from a four-dimensional Wilson-Dirac operator with a negative Wilson mass  $m_0$  and calculates its eigenvalues. For  $m_0$  small and positive, the number of positive eigenvalues is equal to that of negative ones. When  $m_0$  increases, a level might cross from positive to negative or vice versa. When this happens, the gauge field is regarded to have a net topological charge  $|Q| = 1$ . Then the overlap determinant is exactly zero by construction. This definition of lattice topology and zero mode do depend on, for instance, the Wilson parameters  $r$  and  $m_0$ . However, the zero eigenvalue is exact, independent of the lattice spacing  $a$  and volume  $V$ .

The domain-wall formulation can be regarded as an approximation to the overlap formalism [3]. Indeed, in the limit of  $L_s \rightarrow \infty$ , one recovers the overlap formalism apart from some unimportant discretization effect in the fifth dimension. For a fixed gauge configuration and Wilson mass  $m_0$ , if the overlap determinant is zero,  $H_{DW}$  has an exact zero mode in the limit of  $L_s \rightarrow \infty$ .

In short, in a background gauge field, if the hermitian Wilson-Dirac operator has a level crossing, the gauge field is considered to have a nontrivial topology. Edwards, Heller, and Narayanan have done extensive studies of the topological properties of lattice gauge configurations in this way [10]. In a topologically-nontrivial background thus defined, the domain-wall Dirac operator with a finite  $L_s$  has small eigenvalues, nonvanishing only because of the finite wall separation. In the remainder of this paper, we are mainly interested in such domain-wall effects on the fermion zero-mode. We *define* the smallest eigenvalues of the hermitian domain-wall operator  $H_{DW}$  as the wall-induced effective fermion mass.

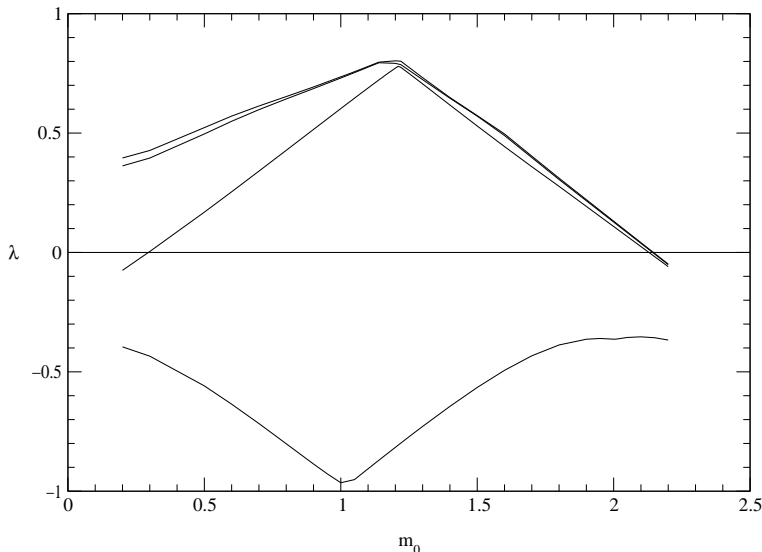


FIG. 2. Smallest eigenvalues of the hermitian Wilson-Dirac operator in a smooth (anti)instanton field described in the text.

As a first nontrivial example, we have shown in Figs. 2 and 3 the results in a smooth instanton field configuration on an  $8^4$  lattice. A similar study has been reported in Refs. [3,10,11]. In our case, the instanton configuration was generated according to the prescription in Ref. [12]: The size of the instanton  $\rho_0$  is 10 and the cutoff parameter  $r_{\max}$  is 3. The flow of the small eigenvalues of the hermitian Wilson-Dirac operator is shown in Fig. 2. A level crossing from positive to negative is seen at  $m_0 = 0.3$ . Four separate crossings in the opposite direction happen near  $m_0 = 2.2$ . Only three of the crossings are plotted. In the overlap formalism, the Dirac operator has an exact zero eigenvalue in the region between the crossings.

The lowest eigenvalue of the hermitian domain-wall Dirac operator  $H_{DW} = \gamma_5 P_s D$  is shown in logarithmic scale in Fig. 3. The overall profile of the eigenvalue as a function of  $m_0$  is similar to the free case in Fig. 1. For a fixed  $L_s$ , the smallest eigenvalue occurs at around  $m_0 = 1.3$ , shifted upward from  $m_0 = 1$ . This shift reflects the renormalization of

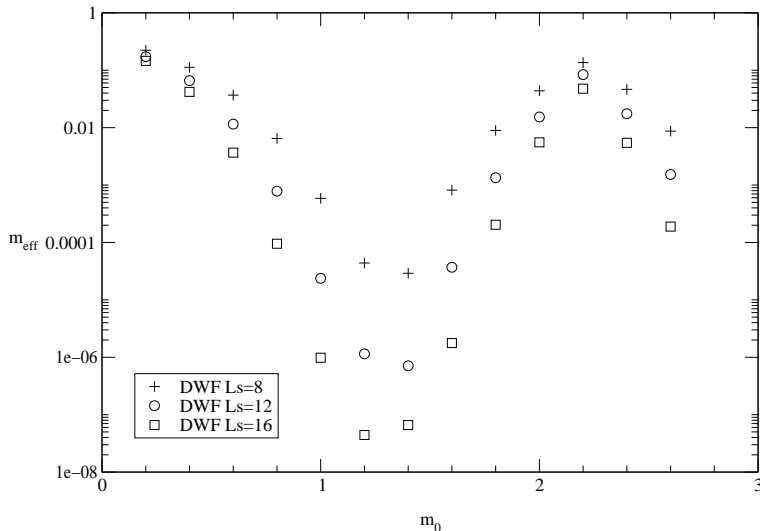


FIG. 3. Effective quark mass induced by domain walls in the same smooth instanton field as studied in Fig. 2.  $L_s$  is the number of lattice sites in the fifth direction.

the Wilson mass in the presence of the external gluon field. As  $m_0$  deviates from  $m_0 = 1.3$ , the domain-wall effects grow stronger. For a fixed  $m_0$ , the effective fermion mass decreases exponentially as  $L_s$  increases from 8 to 12 and 12 to 16.

Our result is quantitatively consistent with the chiral condensate  $\langle \bar{\psi}\psi \rangle$  calculation in Ref. [6]. For instance, at  $L_s = 10$  and  $m_0 = 1.2$ , we have  $m_{\text{eff}} \sim 7 \times 10^{-6}$ . We expect then  $\langle \bar{\psi}\psi \rangle$  grows like  $1/m_f$  as the explicit quark mass parameter  $m_f$  reduces to  $\sim 10^{-5}$ . For a fixed  $m_f = 5 \times 10^{-4}$  and  $L_s = 10$ , there is a window in  $m_0 \sim [0.9, 1.6]$  in Fig. 3 where the induced quark mass  $m_{\text{eff}}$  is smaller than  $m_f$ . Hence we expect  $\langle \bar{\psi}\psi \rangle$  is approximately independent of  $m_0$  there. At  $m_0 = 0.75$ , the effective quark mass is about  $10^{-3}$  with  $L_s = 12$ . We expect the chiral condensate to have little sensitivity on  $m_f$  when  $m_f > 10^{-3}$ . All of the above are in accordance with those reported in Ref. [6].

A smooth instanton on the lattice is far from a typical equilibrium gauge configuration entering in the Feynman path integral. A more realistic study of the induced quark masses requires gauge configurations with quantum fluctuations fully included. In the following, we work on a set of Monte Carlo configurations generated on a four-dimensional  $8^4$  lattice and with  $\beta = 6$ . The physical volume is somewhat small, but we suspect that the domain-wall effects have a weak dependence on it.

We pick a lattice configuration in which the lowest eigenvalue of the hermitian Wilson-Dirac operator crosses from the positive to the negative at  $m_0$  near 0.9. In Fig.4, we have shown the flow of the lowest few eigenvalues as a function of  $m_0$ . Between  $m_0 = 2.35$  and 2.45, four levels cross from the negative to positive region. Although not shown explicitly, six level crossings occur at around  $m_0 = 4$ . As pointed out in Ref. [10], the hermitian Wilson-Dirac operator is symmetric with respect to  $m_0 = 4$  and hence the flow diagram has the same symmetry. According to the overlap fermion formalism, the Neuberger-Dirac operator in the above gauge background has one zero eigenvalue when  $m_0$  is in the interval  $[0.9, 2.35]$ , three zero eigenvalues in  $[2.45, 4]$ , three again in  $[4, 5.55]$ , and finally one in  $[5.65, 7.1]$ .

In Fig.5, we have shown the smallest eigenvalue of the hermitian domain-wall Dirac

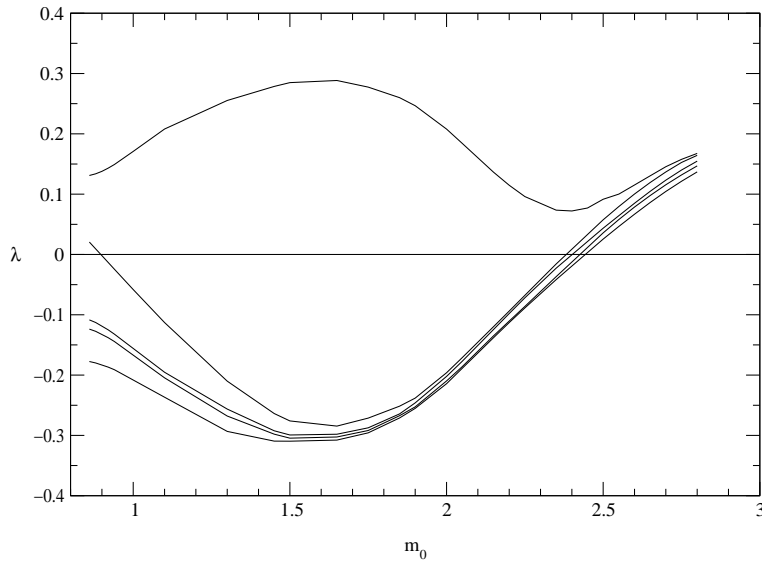


FIG. 4. Eigenvalues of the hermitian Wilson-Dirac operator as a function of the negative Wilson mass  $m_0$  in a topological gauge configuration generated on an  $8^4$  lattice and at  $\beta = 6.0$ .

operator  $H_{DW}$ . Different symbols correspond to three different  $L_s = 8$  (pluses), 12 (circles), and 16 (squares). Over a large region of  $m_0$ , the effective quark mass decreases exponentially in  $L_s$ , as is clear from the approximate equal spacings between pluses, circles, and squares. The fastest decay occurs at  $m_0$  around 2.0, compared with 1.0 in the free case and 1.3 in the smooth instanton field. The wall effects become strong again near  $m_0 = 2.7$  beyond which we find four small eigenvalues (not shown). To our surprise, this transition point to the doubler region is at higher  $m_0$  compared with the prediction from the spectral flow of the hermitian Wilson-Dirac operator. This may indicate some subtle differences between the eigenvalues of the transfer matrix in the domain-wall formalism and those of the hermitian Wilson-Dirac operator in the overlap formalism.

The important point about Fig.5 is that the magnitude of the effective mass is much enhanced relative to the case of the smooth instanton configuration. With a best choice of  $m_0$  near 2.0, the domain-wall Dirac operator has the smallest eigenvalue  $(3 \sim 4) \times 10^{-4}$  at  $L_s = 16$ . For the same  $L_s$  and with  $m_0$  of 1.3, the smooth instanton configuration yields an eigenvalue  $\sim 10^{-8}$ . This dramatic increase of the effective mass comes from the ultraviolet fluctuations. As we will discuss further below, the ultraviolet fluctuations at strong coupling can cause great trouble for the domain-wall formalism. In Fig. 6, we have shown the smallest eigenvalue of  $H_{DW}$  in another topological gauge configuration. The result is qualitatively similar to that in Fig. 5. In particular, for  $L_s = 16$  and  $m_0 = 2.0$ , the induced quark mass is around  $10^{-4}$ .

Since the effective quark mass depends on particular gauge fields, it is useful to get an average over an ensemble of gauge configurations. For this purpose, we have generated a set of 150 configurations on a  $8^4$  lattice at  $\beta = 6.0$ . By studying the spectral flow of the hermitian Wilson-Dirac operators, we found 12 topologically-nontrivial configurations. The second column in Table I shows  $m_0$  at which the first level crossing occurs. All the crossing points are entirely concentrated in the interval between 0.8 and 1, a fact consistent with a

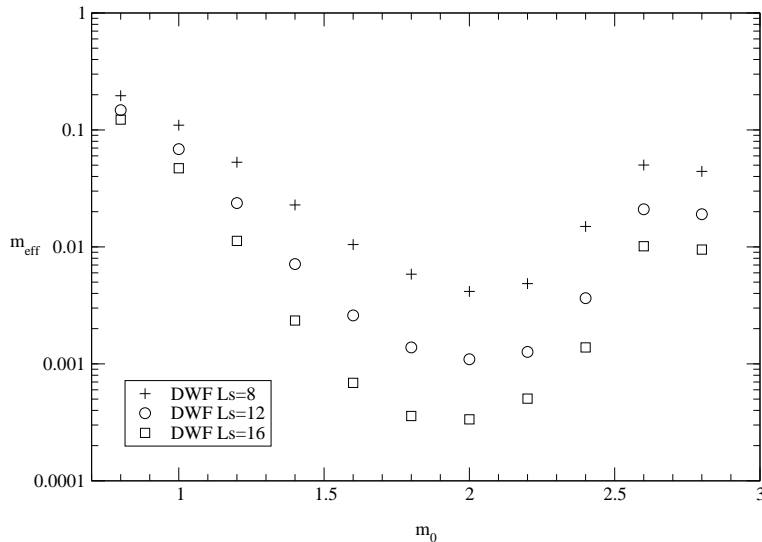


FIG. 5. Effective quark mass induced by the domain walls in the same topological configuration as studied in Fig. 4.

similar study in a slightly larger lattice  $8^3 \times 16$  [10]. We proceed to calculate the lowest eigenvalue of the hermitian domain-wall Dirac operator with  $L_s = 8, 12$ , and  $16$  at  $m_0 = 1.8$ . The result is shown as the remaining columns in Table 1. We find the average effective quark mass at  $L_s = 16$  is  $8(4) \times 10^{-4}$ . The dependence of the average effective mass in  $L_s$  is consistent with the exponential within the error.

Our result can be compared with a previous study of the wall-induced quark mass using the Gell-Mann-Oakes-Renner relation on a  $16^3 \times 32$  lattice at the same value of  $\beta$  [7]. In the domain-wall formulation, the quenched chiral condensate is related to the pion susceptibility  $\chi_\pi$  [7] by

$$\langle \bar{\psi}\psi \rangle = (m_f + m_{\text{eff}}^{\text{GMOR}})\chi_\pi + b \quad (3)$$

where  $b$  is a constant vanishing in the  $L_s \rightarrow \infty$  limit. The effective quark mass  $m_{\text{eff}}$  can be extracted from  $m_f$ -dependence of the condensate and  $\chi_\pi$ . For  $L_s = 16$  and  $m_0 = 1.8$ , an extrapolation to  $m_f = 0$  limit yields  $m_{\text{eff}}^{\text{GMOR}} = 0.012$ . Note that the smallest  $m_f$  at which the data is taken is  $0.01$ .

To understand the physical significance of  $m_{\text{eff}}^{\text{GMOR}}$ , we recall the spectral version of the GMOR relation in the overlap formulation [13]:

$$\langle \bar{\psi}\psi \rangle = m_f \chi_\pi = m_f \left( \frac{|Q|}{m_f^2 V} + \frac{1}{V} \sum_i \frac{2(1 - \lambda_i^2)}{\lambda_i^2 + m_f^2} \right), \quad (4)$$

where  $\pm\lambda_i$  are a conjugating pair of eigenvalues of  $(\gamma_5 D_{\text{ov}})^2$  ( $D_{\text{ov}} =$  overlap Dirac operator). The first term signifies the contribution from the topological zero modes; for sufficiently large volume  $V$  and/or large  $m_f$ , this topological charge term is negligible. The second term measures the chiral symmetry breaking effects on the conjugating pairs of eigenvalues. In the study quoted above [7], the topological charge term is insignificant even at the smallest

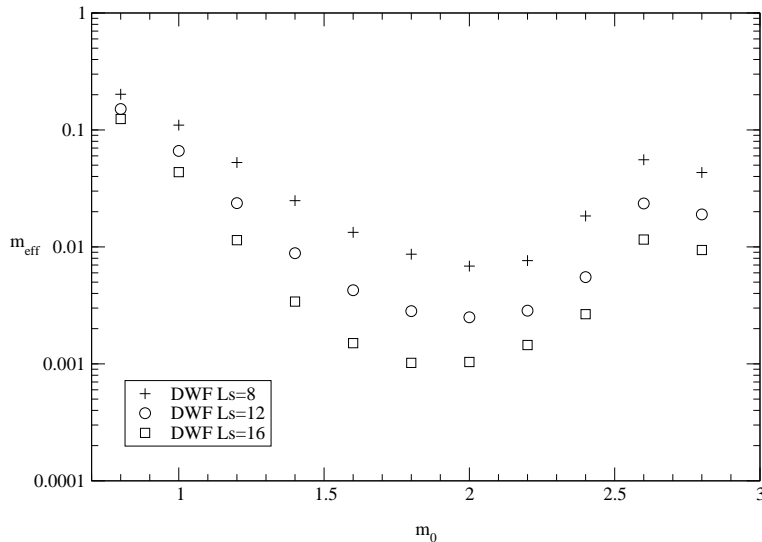


FIG. 6. Same as Fig. 5, but for a different topologically nontrivial configuration.

$m_f = 0.01$ , and the extracted  $m_{\text{eff}}^{\text{GMOR}}$  undoubtedly measures the explicit chiral-symmetry breaking effects in conjugating pairs of eigenvalues as induced by the domain walls.

One can push the quenched calculation in Ref. [7] to the limit  $m_f = 0$ . In this case, both the chiral condensate  $\langle \bar{\psi}\psi \rangle$  and pion susceptibility are dominated by the zero modes. The quark mass obtained from the ratio of the two observables is just the smallest eigenvalue of the Dirac operator in the topologically-nontrivial configurations. Therefore in the quenched chiral limit, the effective quark mass determined from the GMOR relation coincides with what we have considered in this paper. To be sure, the effective mass defined from the effects on the fermion zero modes is not the same as the one defined from the effects on the conjugating pairs of eigenvalues. Nonetheless, both definitions shall be consistent within a factor of order unity. In this spirit, our average effective quark mass  $8(4) \times 10^{-4}$  is indeed in accordance with  $1.2 \times 10^{-3}$  from Ref. [7].

To be completely sure about the consistency of the two approaches, further numerical studies are needed. For instance, along the line of study in Ref. [7] one can attempt to subtract the zero-mode contribution to the chiral condensate and pion susceptibility, and then both quantities can be measured in the  $m_f \rightarrow 0$  limit. On the other hand, the present study can be repeated at a larger physical volume; a  $16^3 \times 32$  lattice will be more suitable for comparison.

We finally return to the central question of the domain-wall fermion formalism: How large an  $L_s$  is needed for a practical simulation? Clearly, the results for the free field or artificially smooth gauge fields are of no help here. The answer depends on the size of quantum fluctuations. For large values of  $\beta$  (and perhaps small physical volumes as well), such as the case we have presented, one can work with  $L_s = 12$  or  $16$  and keep the induced quark mass under control. However, in going to smaller  $\beta$  and larger physical volume, level crossing happens continuously in a region of  $m_0$  above some critical value [10]. From Figs. 5 and 6, we expect that if a level crossing occurs slightly before the  $m_0$  where the domain-wall Dirac operator is defined, the wall-induced quark mass will be huge. [When the level crossing



Configuration Number	Crossing in $m_0$	$m_{\text{eff}}(L_s = 8)$	$m_{\text{eff}}(L_s = 12)$	$m_{\text{eff}}(L_s = 16)$
14	0.916	6.777e-03	1.745e-03	5.014e-04
38	0.874	8.663e-03	2.822e-03	1.019e-03
42	0.876	6.104e-03	1.694e-03	5.601e-04
45	0.897	5.849e-03	1.382e-03	3.584e-04
58	0.945	9.188e-03	2.607e-03	8.037e-04
82	0.862	6.356e-03	1.718e-03	5.298e-04
92	0.901	1.002e-02	3.619e-03	1.471e-03
98	0.853	5.543e-03	1.432e-03	4.189e-04
101	0.842	5.948e-03	2.395e-03	1.449e-03
129	0.845	4.525e-03	1.094e-03	3.066e-04
133	0.877	7.554e-03	2.276e-03	7.677e-04
147	1.003	1.252e-02	4.091e-03	1.447e-03
$\overline{m_{\text{eff}}}$		0.0074(22)	0.0022(9)	0.0008(4)

TABLE I. Average effective mass for the topologically nontrivial configurations

happens slightly above  $m_0$ , the chiral symmetry breaking effects in the conjugation pairs of eigenvalues is expected to be strong. Again this leads to a large effective quark mass.] Then the average effective quark mass can be strongly influenced by this type of accidental configurations depending on the frequency they occur. The level crossings at large  $m_0$  reflect strong quantum fluctuations at the scale of the lattice spacing [10]. Therefore, it is not surprising that at  $\beta = 5.7$ , one needs to have very large  $L_s$  (30 to 40) to keep  $m_{\text{eff}}$  small; of course, this is the price that one has to pay to keep the physical volume large.

To summarize, we have studied the induced quark mass resulted from the finite domain wall separation by diagonalizing the hermitian domain-wall Dirac operator in topologically nontrivial configurations. We find the quantum fluctuation strongly enhances the domain-wall effects. However, the effective mass does show an exponential decay as a function of  $L_s$ . Our result on an  $8^4$  lattice with  $\beta = 6$  is consistent with the effective fermion masses from the GMOR relation, although a detailed analysis shows that the two definitions of the effective mass are not the same. Finally, we comment on the size of  $L_s$  needed in a practical Monte Carlo simulation.

## ACKNOWLEDGMENTS

We thank N. Christ, R. Edwards, and J. Negele for useful discussions related to the subject of this paper. The numerical calculation reported here was performed on the Calico Alpha Linux Cluster at the Jefferson Laboratory, Virginia. This work is supported in part by funds provided by the U.S. Department of Energy (D.O.E.) under cooperative agreement DOE-FG02-93ER-40762.

## APPENDIX A: EIGENVALUES OF FREE DOMAIN-WALL FERMION

The domain-wall induced fermion mass in the free case was first calculated by Shamir [2] using Green's function approach. Vranas stated in his paper [5] that he obtained the same result by diagonalizing the domain-wall Dirac operator without showing the actual calculation. An explicit derivation of  $m_{\text{eff}}$  in the  $m_f = 0$  case was later provided by Neuberger [14]. Here we show a complete derivation with the inclusion of  $m_f$ .

The domain-wall Dirac operator in the free field limit in momentum space can be written as:

$$D = i\bar{p} + M^+P_+ + M^-P_- , \quad (\text{A1})$$

where  $P_{\pm} = \frac{1}{2}(1 \pm \gamma_5)$  and  $\bar{p} = \gamma_{\mu} \sin p^{\mu}$ . Mass matrices  $M^{\pm}$  are defined as

$$\begin{aligned} (M^+)_{ss'} &= \delta_{s+1,s'} - b(p)\delta_{s,s'} - m_f\delta_{s,N_s}\delta_{s',1} , \\ (M^-)_{ss'} &= \delta_{s-1,s'} - b(p)\delta_{s,s'} - m_f\delta_{s,1}\delta_{s',N_s} \quad (s, s' = 1, \dots, N_s) , \end{aligned} \quad (\text{A2})$$

where  $b(p) = 1 - m_0 + \sum_{\mu}(1 - \cos p_{\mu})$  and  $m_f$  is the explicit fermion mass. Our goal is to calculate the smallest eigenvalue of the bilinear hermitian domain-wall Dirac operator

$$DD^{\dagger} = \bar{p}^2 + M^+M^-P_+ + M^-M^+P_- . \quad (\text{A3})$$

Since  $M^+M^-$  and  $M^-M^+$  have the same eigenvalue spectrum, it is sufficient to consider

$$M^+M^- = \begin{pmatrix} b^2 + 1 & -b & 0 & \dots & m_fb \\ -b & b^2 + 1 & -b & \dots & 0 \\ \vdots & & & \ddots & \\ m_fb & \dots & 0 & -b & b^2 + m_f^2 \end{pmatrix} . \quad (\text{A4})$$

The second to  $(N_s - 1)$ -th row of the secular equation  $(M^+M^-)_{ss'}\Psi_{s'} = \lambda^2\Psi_s$ , or,

$$(b^2 + 1)\Psi_s - b(\Psi_{s-1} + \Psi_{s+1}) = \lambda^2\Psi_s , \quad (\text{A5})$$

is solved by  $\Psi_s = \exp[\pm\alpha s]$  ( $s = 1, \dots, N_s$ ), provided  $\lambda$  and  $\alpha$  satisfy

$$-2b \cosh(\alpha) + (b^2 + 1 - \lambda^2) = 0 . \quad (\text{A6})$$

The first and the last rows of the secular equation can be satisfied by a linear combination of exponential solutions,  $\Psi_s = \exp[-\alpha(s-1)] + A \exp[-\alpha(N_s-s)]$ , where  $A$  is a constant to be determined:

$$\begin{aligned} (b^2 + 1 - \lambda^2)(1 + Ae^{-\alpha(N_s-1)}) - b(e^{-\alpha} + Ae^{-\alpha(N_s-2)}) + m_fb(e^{-\alpha(N_s-1)} + A) &= 0 , \\ (b^2 + m_f^2 - \lambda^2)(e^{-\alpha(N_s-1)} + A) - b(e^{-\alpha(N_s-2)} + Ae^{-\alpha}) + m_fb(1 + Ae^{-\alpha(N_s-1)}) &= 0 . \end{aligned} \quad (\text{A7})$$

Using Eq. (A6) to eliminate  $\lambda$  from the above, we get

$$\begin{aligned} 2 \cosh(\alpha)(1 + Ae^{-\alpha(N_s-1)}) - (e^{-\alpha} + Ae^{-\alpha(N_s-2)}) + m_f(e^{-\alpha(N_s-1)} + A) &= 0 , \\ (2 \cosh(\alpha) - (1 - m_f^2)/2b)(e^{-\alpha(N_s-1)} + A) & \\ - (e^{-\alpha(N_s-2)} + Ae^{-\alpha}) + m_f(1 + Ae^{-\alpha(N_s-1)}) &= 0 . \end{aligned} \quad (\text{A8})$$

Eliminating A from Eq. (A8) and rearranging terms, we have

$$e^{2\alpha} - e^\alpha/b - m_f^2(1 - e^\alpha/b) + 2m_f e^{-\alpha N_s}(e^{2\alpha} - 1) + m_f^2 e^{-\alpha(2N_s-2)}(e^\alpha - 1/b) - e^{-\alpha 2N_s}(1 - e^\alpha/b) = 0. \quad (\text{A9})$$

In the  $N_s = \infty, m_f = 0$  limit,  $e^\alpha = 1/b$ . Assuming  $e^\alpha = 1/b + \delta$  and keeping terms linear in  $\delta$ , we find

$$\delta \sim -(m_f + b^{N_s})^2(1 - b^2)/b. \quad (\text{A10})$$

Finally, substituting  $e^\alpha = 1/b + \delta$  into Eq. (A6), we get the eigenvalue,

$$\lambda^2 = b^2 + 1 - b(e^\alpha + e^{-\alpha}) \sim -b(1 - b^2)\delta = (1 - b^2)^2(m_f + b^{N_s})^2,$$

or  $\lambda = (1 - b^2)(m_f + b^{N_s})$ , as quoted in Ref. [2].

## REFERENCES

- [1] D. B. Kaplan, Phys. Lett. B **288**, 342 (1992).
- [2] Y. Shamir, Nucl. Phys. **B406**, 90 (1993);  
Y. Shamir, Nucl. Phys. **B417**, 167 (1994);  
V. Furman and Y. Shamir, Nucl. Phys. **B439**, 54 (1995).
- [3] R. Narayanan and H. Neuberger, Phys. Lett. B **302**, 62 (1993);  
R. Narayanan and H. Neuberger, Nucl. Phys. **B412**, 574 (1994);  
R. Narayanan and H. Neuberger, Nucl. Phys. **B443**, 305 (1995);  
H. Neuberger, Phys. Lett. B **417**, 141 (1998).
- [4] T. Blum and A. Soni, Phys Rev. D **56**, 174 (1997);  
T. Blum and A. Soni, Phys. Rev. Lett. **79**, 3595 (1997);  
T. Blum, A. Soni, and M. Wingate, Phys. Rev. D **60**, 114507 (1999).
- [5] P. Vranas, Nucl. Phys. Proc. Supp. **63**, 605 (1998);  
P. Vranas, Phys. Rev. D **57**, 1415 (1998);  
P. Vranas et al, Nucl. Phys. Proc. Supp. **73**, 456 (1999);  
P. Vranas et al, hep-lat/9911002.
- [6] P. Chen et al., Presented at 29th Intl. Conf. on High-Energy Physics (ICHEP 98),  
Vancouver, Canada, 23-29 Jul 1998. In \*Vancouver 1998, High energy physics, vol. 2\*  
1802-1808. hep-lat/9812011;  
P. Chen et al., Nucl. Phys. Proc. Suppl. **73** 204, 207, 405 (1999)
- [7] G. R. Fleming, to appear in the proceedings of LATTICE '99, hep-lat/9909140.
- [8] M. Atiyah and I. M. Singer, Ann. Math. **93**, 139 (1971).
- [9] G. 't Hooft, Phys. Rev. Lett. **37**, 8 (1976); Phys. Rev D **14**, 3432 (1976).
- [10] R.G. Edwards, U. M. Heller and R. Narayanan, Nucl. Phys. **522**, 285 (1998);  
R.G. Edwards, U. M. Heller and R. Narayanan, Nucl. Phys. **535**, 403 (1998).
- [11] R.G. Edwards, U. M. Heller and R. Narayanan, hep-lat/0001013.
- [12] P. Chen et al., Phys. Rev. D **59** 054508 (1999).
- [13] R. G. Edwards, U. M. Heller, and R. Narayanan, Phys. Rev. D **59**, 094510 (1999).
- [14] H. Neuberger, Phys. Rev. D **57**, 5417 (1998).